**Journal of Nuclear Medicine, published on April 7, 2022 as doi:10.2967/jnumed.121.263357**

**Title:** Brown adipose tissue: a protective mechanism against “pre-prediabetes”?

**Running Title: Active BAT-associated metabolic changes**

**Authors:** John P. Crandall[1], Tyler J. Fraum[1], Richard L. Wahl[1]

**Affiliations:** [1]Mallinckrodt Institute of Radiology, Washington University School of Medicine, St. Louis, MO, USA

**Corresponding Author**:
Richard L. Wahl
Mallinckrodt Institute of Radiology
Washington University School of Medicine
510 S. Kingshighway Blvd
Campus Box 8131
St. Louis, MO 63110
Phone: (314) 362 – 7100
Fax: (314) 361 – 5428
Email: *rwahl@wustl.edu*

**First Author:**
John P. Crandall
Mallinckrodt Institute of Radiology
Washington University School of Medicine
510 S. Kingshighway Blvd
Campus Box 8131
St. Louis, MO 63110
Phone: (314) 747 – 5561
Fax: (314) 361 – 5428
Email: *jcrandall@wustl.edu*

**Financial Support:** None

**Word Count**: 6455

## ABSTRACT

Brown adipose tissue (BAT) is present in a significant number of adult humans and has been postulated to exert beneficial metabolic effects. Lean, non-diabetic patients undergoing clinical positron emission tomography (PET)/computed tomography (CT) imaging are more likely to exhibit incidental BAT activation. The aim of this study was to assess metabolic changes associated with the cold-activation of BAT and to compare baseline blood metabolites in participants with varying amounts of active BAT.

*Methods:* Serum blood samples were collected from healthy adult volunteers (body mass index 18.0-25.0 and age≤35 years) before and after 2 h cold exposure. $^{18}$F-flurodeoxyglucose (FDG) PET/CT imaging was performed immediately following cold exposure. Activated BAT was segmented and fasting glucose, insulin, lipid, and other blood metabolite levels were correlated with volume and intensity of active BAT. Using a median cutoff, subjects were classified as $BAT_{HIGH}$ or $BAT_{LOW}$.

*Results.* A higher volume of activated BAT was associated with significantly higher pre-cooling glucose and insulin levels ($P<0.001$ for each). Pre-cooling thyroid stimulating hormone (TSH) and triglyceride levels were significantly higher in the $BAT_{HIGH}$ than in the $BAT_{LOW}$ group ($P=0.002$ and $P<0.001$, respectively). Triglyceride levels tended to increase over the cooling period in both BAT groups, but increased significantly more in the $BAT_{HIGH}$ group (15.7±13.2 md/dl; $P<0.001$) than in the $BAT_{LOW}$ group (4.5±12.2 mg/dl; $P=0.061$).

*Conclusions.* These findings may indicate that BAT is recruited to counteract incipient “pre-prediabetic” states, potentially serving as a first-line protective mechanism against very early metabolic or hormonal variations.

## INTRODUCTION

Brown adipose tissue (BAT) utilizes a variety of metabolic substrates to produce heat in mammals and so constitutes a potential target for the treatment of obesity and other metabolic disorders (*1*). White adipose tissue (WAT) stores energy as triacylglycerols, which can be released as non-esterified fatty acids (NEFA) for energy consumption by metabolically active organs. BAT uses fatty acids released from intracellular triglyceride stores for beta oxidation to generate heat by a process known as adaptive thermogenesis (*2*).

The presence of BAT in adult humans was initially recognized mainly on $^{18}$F-fluorodeoxyglucose (FDG) positron emission tomography (PET)/computed tomography (CT) examinations performed for oncologic indications (*3,4*). FDG PET has since become the most commonly used technique for the *in vivo* detection of cold-activated BAT in humans (*5,6*). Studies using PET with FDG and/or fatty-acid tracers have demonstrated that BAT consumes glucose and fatty acids (*7-9*).

### Glucose Metabolism

Two primary pathways are known to regulate BAT glucose metabolism: adrenergic and insulin signaling (*1*). Upon sympathetic nervous system activation, norepinephrine is released, which binds to adrenergic receptors ($\beta_1$-, $\beta_2$- and $\beta_3$- adrenoceptors) expressed on BAT cell surfaces, causing an increase in cytosolic cyclic adenosine monophosphate (cAMP) levels (*10*). The result is an increase in glucose transporter (GLUT) 1 transcription and, via activation of the mammalian target of rapamycin (mTOR) complex 2, the translocation of this newly-synthesized GLUT1 to the cell membrane (*11*). Alternatively, insulin binds to BAT insulin receptors, phosphoinositide 3-kinases (PI3K) phosphorylate protein kinase B (PKB), inducing the translocation of GLUT4 to the cell membrane. Glucose, having been taken up by BAT cells using either pathway, is utilized for either glycolysis, maintaining fatty acid oxidation, or activation of uncoupling protein 1 (UCP1) via de-novo lipogenesis and fatty-acid synthesis (*2*).

The regulation of glucose by activated BAT may have important therapeutic implications, as exposure to cold has been shown to reverse glucose intolerance and insulin resistance in animal models (*12-14*). Cold acclimation may also result in increased fractional uptake in BAT (*15*). Observational human studies have indicated that the presence of active BAT is associated with lower glucose levels and a decreased risk of diabetes (*16-18*). However, the role of BAT in whole-body glucose consumption remains unclear since several prospective studies have indicated a minimal contribution by BAT to systemic glucose utilization (*8,19*). Still, others have shown a protective effect of BAT against diabetes (*20*).

**Lipid Metabolism**

Current evidence indicates lipid metabolism in humans is modulated, at least to some degree, by BAT. BAT activation has been correlated with cold-induced increases in WAT lipolysis and NEFA oxidation, indicating that NEFAs are mobilized from WAT in order to fuel activated BAT. It has been hypothesized that increased BAT activity or volume increases uptake of NEFA in BAT, improving overall lipid metabolism (*12,21*). A recent retrospective study found that non-stimulated BAT was associated with lower concentrations of circulating triglycerides (*22*). Rodent studies have demonstrated the clearance of triglyceride-rich lipoproteins and cholesterol from circulation by BAT (*12,23*) and have even seemed to demonstrate that active BAT modulates fuel selection in non-BAT organs (*24*). Even during fasting and postprandial conditions, BAT has been shown to take up significant amounts of circulating free fatty acids in mice (*25*). However, the practical implications of active BAT on lipid metabolism in humans remain unclear (*26,27*).

The primary aim of this study was to assess if there are differences in baseline glucose, insulin, lipid, and other metabolite levels between subjects with varying amounts of cold-activated BAT. A secondary aim was to evaluate changes in these blood markers between pre-cooling and post-cooling serum blood samples. An additional aim was to assess how different

lifestyle parameters are associated with BAT volume. These data were collected as part of a prospective study assessing the repeatability of BAT activity levels on FDG PET/CT (*28*).

## MATERIALS AND METHODS

This prospective study was approved by the Washington University Institutional Review Board. All subjects provided written informed consent prior to participation. Between March, 2016, and January, 2020, 34 healthy volunteers were enrolled and underwent FDG PET/CT imaging following a cooling procedure intended to activate BAT (subject characteristics provided in Table 1). Median FDG uptake time was 61.0 min with a range of 59.0 – 76.6 min. Median blood glucose, measured immediately prior to FDG administration, was 78 mg/dl and ranged from 58 – 103 mg/dl. Since younger age and lower body mass index (BMI) have been shown to correlate with higher amounts of metabolically active BAT (*7,29,30*), healthy adult volunteers ages 18 – 35 with a BMI between 18 and 25 were eligible for this study. Furthermore, as drugs targeting the sympathetic nervous system (e.g., nicotine, beta-blockers, and amphetamines) can interfere with BAT activation (*31*), individuals with a history of consuming these agents were excluded. A complete list of inclusion and exclusion criteria can be found in Supplemental Table 1. Subjects were recruited using flyers posted at various locations on the Washington University in St. Louis medical campus.

### Subject Preparation

A schematic representation of the imaging visit is shown in Figure 1. All subjects were instructed to fast for at least 6 hours prior to imaging and to avoid high-carbohydrate and high-fat foods. Subjects were also asked to avoid cold exposure and to refrain from exercise during the 24 h period before the imaging sessions. In order to prevent premature BAT activation, subjects were kept warm for a 60 minute period, using warmed blankets, before the start of the cold-exposure procedure. During this period, the pre-cooling blood sample was drawn for metabolite analysis.

Following the preparatory phase, participants were outfitted in a cooling suit (CureWrap; MRTE Advanced Technologies; Yavne, Israel) that circulates chilled water at a set temperature.

**Lifestyle Interview**

During the preparatory phase, subjects were asked a series of questions in order to assess the impact of lifestyle on BAT activity. Volunteers were asked to describe any specific diet they followed within the year prior to the study and to report any dietary supplements they consume regularly. Estimates of weekly caffeine and alcohol intake were also collected. Subjects were asked to describe their normal exercise habits, if any, during the previous year. Exercise descriptions were recorded and coded as 'mostly aerobic', 'mostly anaerobic', or 'combination aerobic/anaerobic'.

**Cooling Protocol**

An individualized cooling protocol was used with a goal of cooling the subject to just above the shivering point (*5*). Initially, the water temperature of the cooling suit was set at 10ºC for all subjects. Subjects were monitored for shivering, both visibly and via electromyogram (electrodes placed over the vastus lateralis, pectoralis major, and latissimus dorsi muscles). If shivering was observed or reported, the water temperature was increased at 0.5ºC increments every 60 s until cessation of shivering was achieved. Oral temperature and blood pressure was measured every 5 min during the cooling procedure. A 185 MBq dose of FDG was administered intravenously after 60 min of cooling. Cooling continued during the 60 minute FDG uptake phase. Immediately prior to FDG PET/CT imaging, subjects were removed from the cooling suit.

**Imaging Protocol**

Imaging and reconstruction parameters are detailed in Supplemental Table 2. All subjects were imaged on a Siemens Biograph 40 PET/CT TruePoint/TrueView scanner (Siemens AG; Erlangen, Germany). In humans, most active BAT depots are located in the supraclavicular and paravertebral regions with additional foci commonly seen in the axillary, intercostal, mediastinal, and perirenal areas. Therefore, PET imaging (three 8 min list-mode acquisitions) was performed

from the skull base to the umbilicus. A low-dose CT (utilizing CareDose tube current modulation) was obtained immediately prior to the PET. The imaging protocol followed the standards set forth by the Uniform Protocols for Imaging in Clinical Trials (UPICT) for FDG PET/CT and the Radiologic Society of North America – Quantitative Imaging Biomarker Alliance's profile for quantitative FDG PET/CT (*32,33*).

**Image Analysis**

Image analysis was performed using MIM version 6.9.3 (MIM Software; Cleveland, OH). Activated BAT was segmented (Fig. 2) and quantified according to the brown adipose reporting criteria in imaging studies (BARCIST) 1.0 recommendations (*5*). Areas known to contain BAT were qualitatively assessed and likely BAT depots identified. Volumes of interest (VOI) were drawn in a slice-by-slice fashion on coronal, fused FDG-PET/CT images, taking care not to include any adjacent normal FDG-avid tissues. Thresholds were then applied to this manual VOI to first remove voxels with lean body mass-adjusted standardized uptake values (SUL) below 1.2 and then to remove voxels with Hounsfield units (HUs) outside of the -190 to -10 range . Thus, the final activated BAT volumes consisted of voxels with SULs above normal background levels and within the fat density range.

The total activated BAT metabolic volume (BMV) was the sum of all segmented BAT volumes. For participants included in the test-retest study (see further below), BMV and the maximum SUL ($SUL_{MAX}$) for each imaging session was analyzed separately. The $SUL_{MAX}$ was defined as the single voxel within all the segmented BAT depots with the greatest FDG uptake. Note that the version of MIM utilized for our analyses employs the James equation for lean body mass computation (*34*). For subjects without visually-detectable BAT, the $SUL_{MAX}$ was instead based on the background activity of the fat in the right supraclavicular fossa, using a spherical region of interest (3.0 cm radius). This region was chosen because the supraclavicular fossa most commonly contains the BAT depot with the most FDG uptake.

**Biological Assays**

Methods used for blood sample analyses are provided in Supplemental Table 3. All tests were performed using either the Cobas ® 6000 or the Cobas ® 8000 (Roche Diagnostics, Basel, Switzerland). Blood sample analyses were performed in the Barnes Jewish Clinical Chemistry Laboratory, which holds College of American Pathologists (CAP) and Clinical Laboratory Improvement Amendments (CLIA) certifications. Please note that lipid data was available for all subjects, while insulin, glucose and other metabolite data was only available for a subset of participants.

**Statistics**

Numeric results are reported as mean (SD) or median (IQR). Subject characteristics were summarized descriptively via means, medians, standard deviations, and ranges, as specified in the text. A subset of participants were included in a test-retest repeatability study (n=29) and underwent the cooling and imaging protocol twice on separate days. Blood samples collected during these visits were pooled with the remaining data and considered as independent samples. Baseline and post-cooling metabolite measurements were compared using paired *t*-tests. Serum metabolite differences between $BAT_{HIGH}$ and $BAT_{LOW}$ groups were assessed using unpaired *t*-tests or Mann-Whitney U tests, depending on group normality. Group normality was assessed using D'Agostino-Pearson tests. Fisher's exact test was used to assess differences between subjects without versus with detectable BAT with respect to demographics and lifestyle assessments. Data analyses were performed using R version 4.0.3 (*http://cran.r-project.org/*) and Excel 2016 (Microsoft Corporation). A *P*-value less than 0.05 was considered significant, unless otherwise indicated. A Bonferroni correction for multiple comparisons was applied when necessary to control for type I errors.

## RESULTS

### Subject Characteristics

During cold exposure, oral temperatures varied by a mean of ±0.4 $^{O}$C. Systolic pressure increased during cooling by a minimum of 8 and a maximum of 42 mm Hg. Diastolic pressure increased during cooling by a minimum of 11 and a maximum of 39 mm Hg. Heart rate increased by 11 – 30 BPM throughout cooling.

Activated BAT was detected in 28 of 34 (82.4%) subjects. Using a median volume cutoff, PET/CT studies showing an activated BMV greater or less than 120 ml were classified as $BAT_{HIGH}$ or $BAT_{LOW}$, respectively. The mean BMV of the $BAT_{LOW}$ group (n=17) was 36.9±29.1 ml and the BMV of the $BAT_{HIGH}$ group (n=17) was 224.3±78.4 ml. There were no substantial differences in age, height, or weight between groups. A significant difference in BMI was found, with $BAT_{HIGH}$ subjects having a higher BMI than $BAT_{LOW}$ subjects ($P$=0.026).

### Insulin and Glucose

Mean baseline insulin and glucose levels were significantly lower in the $BAT_{LOW}$ than in the $BAT_{HIGH}$ group (Table 2). Between baseline and post-cooling samples, mean insulin levels increased by 1.6±1.2 mcu/ml in the $BAT_{LOW}$ group and decreased by 2.7±1.4 mcu/ml in the $BAT_{HIGH}$ group. Baseline glucose and insulin showed significant positive correlations with both BMV and $SUL_{MAX}$ (Figs. 3 and 4). The change in glucose and insulin levels from baseline to post-cooling samples showed significant negative correlations with both BMV and $SUL_{MAX}$. Baseline insulin and glucose were also significantly correlated with one another ($r$=0.67; $P$<0.001), as were the changes in insulin and glucose ($r$=0.51; $P$=0.019).

**Lipids**

Groupwise serum lipid results are shown in Table 3. Baseline total cholesterol, triglycerides, and high density lipoprotein (HDL) were significantly higher ($P$=0.002, $P$<0.001, and $P$=0.004, respectively) in $BAT_{LOW}$ versus $BAT_{HIGH}$ subjects. The $BAT_{LOW}$ group also showed higher baseline low density lipoprotein (LDL) and non-HDL levels than the $BAT_{HIGH}$ group, though not statistically different. Between baseline and post-cooling blood samples, serum total cholesterol, HDL, non-HDL, and LDL increased significantly for both groups (all $P$-values below 0.01). Serum triglycerides increased significantly between baseline and post-cooling samples for $BAT_{HIGH}$ subjects (15.7±13.2 md/dl; $P$<0.001), but did not increase significantly in the $BAT_{LOW}$ group (4.5±12.2 mg/dl; $P$=0.061).

Baseline triglycerides, cholesterol, and HDL were also significantly correlated with BMV and $SUL_{MAX}$ (Supplemental Figs. 1 and 2). The change in triglycerides from baseline to post-cooling samples was also significantly correlated with BMV and $SUL_{MAX}$.

**Other Metabolites**

Several additional metabolites showed groupwise differences and varied significantly between baseline and post-cooling blood samples (Table 4). Mean baseline thyroid stimulating hormone (TSH) was significantly lower in the $BAT_{LOW}$ than in the $BAT_{HIGH}$ group ($P$=0.002). Mean baseline sodium, anion gap, urea nitrogen, albumin, and alkaline phosphatase were significantly higher in the $BAT_{LOW}$ than in the $BAT_{HIGH}$ group.

**Lifestyle**

Participants reported engaging in either no strict dietary regimen or adhering to a vegetarian, vegan, gluten-free, low-carbohydrate, or pescatarian diet. $BAT_{LOW}$ subjects were significantly more likely to report observing a controlled diet than $BAT_{HIGH}$ subjects ($P$=0.007). Only 1 of 17 $BAT_{HIGH}$ participants reported following a specific diet (pescatarian), while 8 of 17 $BAT_{LOW}$ subjects reported adhering to a strict diet. The use of dietary supplements also varied between groups, with $BAT_{HIGH}$ subjects reporting either no use of dietary supplements or use of protein, melatonin, biotin, omega-6 fatty acids, or magnesium (8 of 17 subjects), while $BAT_{LOW}$ subjects reported either no diet supplementation or using only a daily multivitamin (7 of 17 subjects). There were no significant differences between groups with respect to self-reported weekly intake of caffeine or alcohol.

Exercise habits also differed between groups. Those who reported not regularly exercising were significantly more likely to have higher BAT volumes (7/17 $BAT_{HIGH}$ versus 0/16 $BAT_{LOW}$; $P$=0.018). Among those who exercised regularly, the self-reported mean number of hours spent exercising per week was 3.4 in the $BAT_{LOW}$ group and 1.9 in the $BAT_{HIGH}$ group ($P$=0.011). Within the $BAT_{LOW}$ group, 1 participant reported engaging in mostly anaerobic exercise, 10 in mostly aerobic exercise, and 6 in exercise that incorporated aerobic and anaerobic elements. Three $BAT_{HIGH}$ subjects reported engaging in mostly anaerobic exercise, 2 in mostly aerobic exercise, and 5 in exercise that was both aerobic and anaerobic.

**DISCUSSION**

Brown adipose tissue has emerged as a potential therapeutic target for obesity and related metabolic diseases. Using a previously-described method, BAT was activated in this study using cold exposure and then imaged using FDG PET/CT. Higher baseline insulin and glucose levels were correlated with higher BMV (Supplemental Fig. 3). Greater declines in insulin and glucose levels following BAT activation were also correlated with higher BMV.

**Glucose and Insulin Activity**

Activated BAT has been shown to act as a glucose sink in both warm and cold conditions (*35,36*), which is consistent with the significant positive correlation seen here between BMV and decreases in glucose and insulin levels during cooling. BAT thermogenesis likely resulted in significant uptake of glucose in BAT, especially in subjects with higher amounts of BAT, consistent with previous studies. However, our results are inconsistent with studies showing increased BAT uptake of glucose during warm conditions, as baseline glucose and insulin were both positively correlated with BMV in our subjects. Retrospective analyses have generally concluded that patients with active BAT are more likely to have lower fasting glucose levels and less likely to be diabetic (*7,16,17,37,38*). Though, as these observational studies consisted mostly of patients undergoing clinical FDG PET/CT, the populations evaluated were mostly much older than the volunteers enrolled in the current study.

**Lipid Metabolism**

The role of BAT in systemic lipid metabolism is supported by previous studies showing the amount of detectable BAT correlates with cold-induced increases in WAT lipolysis and NEFA oxidation, suggesting that BAT activation plays a role in NEFA mobilization from WAT and their oxidative disposal in BAT (*19,21*). Din et al. found that in BAT regions, subjects with higher volumes of activated BAT took up more NEFAs from circulation than subjects with lower volumes of BAT (*39*). It has also been shown that administration of nicotinic acid, an inhibitor of triglyceride lipolysis, suppresses the cold-induced BAT metabolic rate, implying lipolysis is central to BAT thermogenesis (*40*). While it seems clear that BAT relies on lipids to fuel thermogenesis during cold exposure, most studies have not found a corresponding increase in serum or plasma lipid levels (*8,14,19*). One possible explanation for the significant increases we found in circulating lipid levels is that activated BMVs elicited in this study were considerably higher than in most other published work. A higher degree of activation would likely cause a depletion of intracellular fuel and require additional substrates from other sources. This type of

control mechanism over triglyceride metabolism via clearance by BAT has been demonstrated in cold-exposed mice (*12*).

**Early Metabolic Dysfunction**

Orava et al. found BAT to be highly sensitive to stimulation by insulin (*35*). It may be the case in young, healthy adults that higher insulin levels result in routine activation of BAT, which has been shown to increase overall BMV (*15,41*). Free fatty acids, derived from triglyceride lipolysis, are thought to be activators of UCP1. We found higher thermoneutral circulating triglyceride levels in subjects with greater volumes of BAT. This may be another mechanism of routine BAT activation. Additionally, baseline plasma TSH was found to be significantly elevated in subjects with higher amounts of cold-activated BAT. TSH receptors are present in adipose tissue and have been linked to an increase in UCP1 expression in preadipocytes (*42*). This may indicate that increased TSH levels stimulate BAT production. These findings, along with the strong positive correlations between BMV and thermoneutral insulin, glucose, and triglyceride levels, may suggest BAT plays a role in protecting against early stages of insulin resistance ("pre-prediabetes") and hyperlipidemias.

**Metabolic Profile**

Previous studies have tended to show that activated BAT is associated with a healthier metabolic profile (i.e. lower fasting glucose, greater insulin sensitivity, and less likelihood of diabetes, obesity, and cardiometabolic diseases) (*16-18,22,37*). The results of our study show that within a group of young, lean, healthy adults, those with higher BMV had a potentially poorer overall metabolic profile. Higher baseline insulin, glucose, TSH and serum triglycerides were associated with higher BMV. Those with less activated BAT also exercised more (about twice as much per week) and were more likely to report adhering to diets that could be considered healthier. The effect of exercise on BAT is unclear in humans, as relevant studies have produced conflicting results. However, exercise is known to cause secretion of endocrine factors which modulate BAT activity, including cardiac natriuretic peptides (induction of UCP1

expression and mitochondrial biogenesis) (*43*), fibroblast growth factor 21 (FGF21; increased BAT activity) (*44*), and interleukin 6 (IL-6; improved BAT-mediated metabolic homeostasis) (*13*).

Dietary differences are particularly interesting, as certain diet regimens likely include foods known to contain BAT-promoting compounds (*45*). At least part of a vegetarian or vegan diet may contain foods rich in phytochemicals such as capsaicin (*46*) or curcumin (*47*), which have been linked to increased BAT activation. There is also accumulating evidence that eicosapentaenoic acid (EPA) and docosahexaenoic acid (DHA), found abundantly in fish oils (a likely component of a pescatarian diet), may stimulate BAT thermogenesis (*48*) and WAT browning (*49*). It may be somewhat surprising then, that all but one subject who reported adhering to a strict dietary regimen were part of the $BAT_{LOW}$ group. It may be the case that the high BMV exhibited by subjects in the $BAT_{HIGH}$ group who exercised less and consumed less healthy diets played a protective role against the early symptoms of metabolic disorders, which are driven at least in part by lifestyle choices.

**BATokines**

While BAT is hypothesized to shift caloric balance in a net-negative direction, its endocrine effects may be more potent. In animal models, BAT transplants can improve glucose tolerance, increase whole-body insulin sensitivity, and reverse type 1 diabetes (*13,25,50*). These improvements are unlikely the result of caloric expenditure or glucose consumption alone, but appear to be caused by BAT endocrine signaling (*51*). Adipokines released from BAT (BATokines) are substances preferentially released by BAT versus WAT, which may have endocrine effects (*52*). BAT is known to release significant amounts of FGF21 (*53,54*), which has a role in improving glucose intolerance and increasing fatty acid oxidation in the liver (*55*). An increase in insulin-like growth factor 1 (IGF-1) is thought to be mostly responsible for the reversal of diabetes seen in mouse models (*56*). Neuregulin 4 (NRG4) is highly expressed in BAT and its overexpression is correlated with improved glucose tolerance and decreased insulin insensitivity (*57*). BATokines such as these, which are potentially released routinely in people

such as those in the $BAT_{HIGH}$ group, may help to mitigate the impacts of early metabolic and/or hormonal disturbances.

It is important to note that while significant differences in metabolite levels were found between groups with higher and lower activated BAT volumes, almost all metabolite levels detected during this study were within normal ranges. In otherwise healthy individuals, such as those studied here, who present with borderline metabolic results (e.g. high normal insulin or glucose) it would be useful to correlate their levels of BAT activity with clinical outcomes over time. It may also be beneficial to collect additional samples at subsequent time points to assess the short-term impact of cooling and BAT activation on lipid and other metabolite levels.

## CONCLUSION

Our data, performed under conditions that strongly activate BAT, show significant systemic differences between individuals with higher and lower volumes of active BAT. From these data, we believe that BAT may be recruited to counteract incipient “pre-prediabetic” states, potentially serving as a first-line protective mechanism against very early metabolic and hormonal variations.

## DISCLOSURE

The authors have declared that no conflict of interest exists.

## ACKNOWLEDGEMENTS

The work presented here was conducted using the scanning and special services in the MIR Center for Clinical Imaging Research located at the Washington University Medical Center. We also thank Lauren Ash, Jessica Cartier, and Lisa Schmidt for assistance with data collection.

**KEY POINTS**

QUESTION: Is active brown fat associated with a particular metabolic profile in healthy, young adults?

PERTINENT FINDINGS: In a young, otherwise healthy sample of adults, a higher volume of active brown fat was found to be associated with significantly higher pre-activation levels of serum glucose, insulin, TSH, and triglycerides.

IMPLICATIONS FOR PATIENT CARE: Imaging brown fat using FDG PET/CT may help identify patients with very early metabolic abnormalities.

## REFERENCES


**1.** Klepac K, Georgiadi A, Tschop M, Herzig S. The role of brown and beige adipose tissue in glycaemic control. *Mol Aspects Med.* 2019;68:90-100.

**2.** Cannon B, Nedergaard J. Brown adipose tissue: function and physiological significance. *Physiol Rev.* 2004;84:277-359.

**3.** Hany TF, Gharehpapagh E, Kamel EM, Buck A, Himms-Hagen J, von Schulthess GK. Brown adipose tissue: a factor to consider in symmetrical tracer uptake in the neck and upper chest region. *Eur J Nucl Med Mol Imaging.* 2002;29:1393-1398.

**4.** Cohade C, Osman M, Pannu HK, Wahl RL. Uptake in supraclavicular area fat ("USA-Fat"): description on 18F-FDG PET/CT. *J Nucl Med.* 2003;44:170-176.

**5.** Chen KY, Cypess AM, Laughlin MR, et al. Brown Adipose Reporting Criteria in Imaging STudies (BARCIST 1.0): recommendations for standardized FDG-PET/CT experiments in humans. *Cell Metab.* 2016;24:210-222.

**6.** Chondronikola M, Beeman SC, Wahl RL. Non-invasive methods for the assessment of brown adipose tissue in humans. *J Physiol.* 2018;596:363-378.

**7.** Cypess AM, Lehman S, Williams G, et al. Identification and importance of brown adipose tissue in adult humans. *N Engl J Med.* 2009;360:1509-1517.

**8.** Ouellet V, Labbe SM, Blondin DP, et al. Brown adipose tissue oxidative metabolism contributes to energy expenditure during acute cold exposure in humans. *J Clin Invest.* 2012;122:545-552.

**9.** Coolbaugh CL, Damon BM, Bush EC, Welch EB, Towse TF. Cold exposure induces dynamic, heterogeneous alterations in human brown adipose tissue lipid content. *Sci Rep.* 2019;9:13600.

**10.** Blondin DP, Nielsen S, Kuipers EN, et al. Human brown adipocyte thermogenesis is driven by β2-AR stimulation. *Cell Metab.* 2020;32:287-300.e287.

**11.** Albert V, Svensson K, Shimobayashi M, et al. mTORC2 sustains thermogenesis via Akt-induced glucose uptake and glycolysis in brown adipose tissue. *EMBO Mol Med.* 2016;8:232-246.

**12.** Bartelt A, Bruns OT, Reimer R, et al. Brown adipose tissue activity controls triglyceride clearance. *Nat Med.* 2011;17:200-205.

**13.** Stanford KI, Middelbeek RJ, Townsend KL, et al. Brown adipose tissue regulates glucose homeostasis and insulin sensitivity. *J Clin Invest.* 2013;123:215-223.

**14.** Iwen KA, Backhaus J, Cassens M, et al. Cold-induced brown adipose tissue activity alters plasma fatty acids and improves glucose metabolism in men. *J Clin Endocrinol Metab.* 2017;102:4226-4234.

**15.** Blondin DP, Labbe SM, Tingelstad HC, et al. Increased brown adipose tissue oxidative capacity in cold-acclimated humans. *J Clin Endocrinol Metab.* 2014;99:E438-446.

**16.** Ouellet V, Routhier-Labadie A, Bellemare W, et al. Outdoor temperature, age, sex, body mass index, and diabetic status determine the prevalence, mass, and glucose-uptake activity of 18F-FDG-detected BAT in humans. *J Clin Endocrinol Metab.* 2011;96:192-199.

**17.** Jacene HA, Cohade CC, Zhang Z, Wahl RL. The relationship between patients' serum glucose levels and metabolically active brown adipose tissue detected by PET/CT. *Mol Imaging Biol.* 2011;13:1278-1283.

**18.** Becher T, Palanisamy S, Kramer DJ, et al. Brown adipose tissue is associated with cardiometabolic health. *Nat Med.* 2021;27:58-65.

**19.** Blondin DP, Labbe SM, Phoenix S, et al. Contributions of white and brown adipose tissues and skeletal muscles to acute cold-induced metabolic responses in healthy men. *J Physiol.* 2015;593:701-714.

**20.** Chondronikola M, Volpi E, Borsheim E, et al. Brown adipose tissue improves whole-body glucose homeostasis and insulin sensitivity in humans. *Diabetes.* 2014;63:4089-4099.

**21.** Chondronikola M, Volpi E, Børsheim E, et al. Brown adipose tissue activation is linked to distinct systemic effects on lipid metabolism in humans. *Cell Metab.* 2016;23:1200-1206.

**22.** Wang Q, Zhang M, Xu M, et al. Brown adipose tissue activation is inversely related to central obesity and metabolic parameters in adult human. *PLoS One.* 2015;10:e0123795.

**23.** Berbee JF, Boon MR, Khedoe PP, et al. Brown fat activation reduces hypercholesterolaemia and protects from atherosclerosis development. *Nat Commun.* 2015;6:6356.

**24.** Schlein C, Talukdar S, Heine M, et al. FGF21 lowers plasma triglycerides by accelerating lipoprotein catabolism in white and brown adipose tissues. *Cell Metab.* 2016;23:441-453.

**25.** Gunawardana SC, Piston DW. Reversal of type 1 diabetes in mice by brown adipose tissue transplant. *Diabetes.* 2012;61:674-682.

**26.** Blondin DP, Tingelstad HC, Noll C, et al. Dietary fatty acid metabolism of brown adipose tissue in cold-acclimated men. *Nat Commun.* 2017;8:14146.

**27.** M UD, Saari T, Raiko J, et al. Postprandial oxidative metabolism of human brown fat indicates thermogenesis. *Cell Metab.* 2018;28:207-216 e203.

**28.** Fraum TJ, Crandall JP, Ludwig DR, et al. Repeatability of quantitative brown adipose tissue imaging metrics on positron emission tomography with (18)F-fluorodeoxyglucose in humans. *Cell Metab.* 2019;30:212-224.e214.

**29.** Cohade C, Mourtzikos KA, Wahl RL. "USA-Fat": prevalence is related to ambient outdoor temperature-evaluation with 18F-FDG PET/CT. *J Nucl Med.* 2003;44:1267-1270.

**30.** Saito M, Okamatsu-Ogura Y, Matsushita M, et al. High incidence of metabolically active brown adipose tissue in healthy adult humans: effects of cold exposure and adiposity. *Diabetes.* 2009;58:1526-1531.

**31.** Baba S, Tatsumi M, Ishimori T, Lilien DL, Engles JM, Wahl RL. Effect of nicotine and ephedrine on the accumulation of 18F-FDG in brown adipose tissue. *J Nucl Med.* 2007;48:981-986.

**32.** Graham MM, Wahl RL, Hoffman JM, et al. Summary of the UPICT protocol for 18F-FDG PET/CT imaging in oncology clinical trials. *J Nucl Med.* 2015;56:955-961.

**33.** Kinahan PE, Perlman ES, Sunderland JJ, et al. The QIBA profile for FDG PET/CT as an imaging biomarker measuring response to cancer therapy. *Radiology.* 2020;294:647-657.

**34.** Tahari AK, Chien D, Azadi JR, Wahl RL. Optimum lean body formulation for correction of standardized uptake value in PET imaging. *J Nucl Med.* 2014;55:1481-1484.

**35.** Orava J, Nuutila P, Lidell ME, et al. Different metabolic responses of human brown adipose tissue to activation by cold and insulin. *Cell Metab.* 2011;14:272-279.

**36.** Weir G, Ramage LE, Akyol M, et al. Substantial metabolic activity of human brown adipose tissue during warm conditions and cold-induced lipolysis of local triglycerides. *Cell Metab.* 2018;27:1348-1355 e1344.

**37.** Lee P, Greenfield JR, Ho KK, Fulham MJ. A critical appraisal of the prevalence and metabolic significance of brown adipose tissue in adult humans. *Am J Physiol Endocrinol Metab.* 2010;299:E601-606.

**38.** Persichetti A, Sciuto R, Rea S, et al. Prevalence, mass, and glucose-uptake activity of $^{18}$F-FDG-detected brown adipose tissue in humans living in a temperate zone of Italy. *PloS one.* 2013;8:e63391-e63391.

**39.** Din MU, Raiko J, Saari T, et al. Human brown fat radiodensity indicates underlying tissue composition and systemic metabolic health. *J Clin Endocrinol Metab.* 2017.

**40.** Blondin DP, Frisch F, Phoenix S, et al. Inhibition of intracellular triglyceride lipolysis suppresses cold-induced brown adipose tissue metabolism and increases shivering in humans. *Cell Metab.* 2017;25:438-447.

**41.** van der Lans AA, Hoeks J, Brans B, et al. Cold acclimation recruits human brown fat and increases nonshivering thermogenesis. *J Clin Invest.* 2013;123:3395-3403.

**42.** Zhang L, Baker G, Janus D, Paddon CA, Fuhrer D, Ludgate M. Biological effects of thyrotropin receptor activation on human orbital preadipocytes. *Invest Ophthalmol Vis Sci.* 2006;47:5197-5203.

**43.** Hansen D, Meeusen R, Mullens A, Dendale P. Effect of acute endurance and resistance exercise on endocrine hormones directly related to lipolysis and skeletal muscle protein synthesis in adult individuals with obesity. *Sports Med.* 2012;42:415-431.

**44.** Hanssen MJ, Broeders E, Samms RJ, et al. Serum FGF21 levels are associated with brown adipose tissue activity in humans. *Sci Rep.* 2015;5:10275.

**45.** Okla M, Kim J, Koehler K, Chung S. Dietary factors promoting brown and beige fat development and thermogenesis. *Adv Nutr.* 2017;8:473-483.

**46.** Yoneshiro T, Aita S, Kawai Y, Iwanaga T, Saito M. Nonpungent capsaicin analogs (capsinoids) increase energy expenditure through the activation of brown adipose tissue in humans. *Am J Clin Nutr.* 2012;95:845-850.

**47.** Wang S, Wang X, Ye Z, et al. Curcumin promotes browning of white adipose tissue in a norepinephrine-dependent way. *Biochem Biophys Res Commun.* 2015;466:247-253.

**48.** Oudart H, Groscolas R, Calgari C, et al. Brown fat thermogenesis in rats fed high-fat diets enriched with n-3 polyunsaturated fatty acids. *Int J Obes Relat Metab Disord.* 1997;21:955-962.

**49.** Zhao M, Chen X. Eicosapentaenoic acid promotes thermogenic and fatty acid storage capacity in mouse subcutaneous adipocytes. *Biochem Biophys Res Commun.* 2014;450:1446-1451.

**50.** Liu X, Zheng Z, Zhu X, et al. Brown adipose tissue transplantation improves whole-body energy metabolism. *Cell Res.* 2013;23:851-854.

**51.** White JD, Dewal RS, Stanford KI. The beneficial effects of brown adipose tissue transplantation. *Mol Aspects Med.* 2019.

**52.** Lee MW, Lee M, Oh KJ. Adipose tissue-derived signatures for obesity and type 2 diabetes: adipokines, batokines and microRNAs. *J Clin Med.* 2019;8.

**53.** Chartoumpekis DV, Habeos IG, Ziros PG, Psyrogiannis AI, Kyriazopoulou VE, Papavassiliou AG. Brown adipose tissue responds to cold and adrenergic stimulation by induction of FGF21. *Mol Med.* 2011;17:736-740.

**54.** Di Franco A, Guasti D, Squecco R, et al. Searching for classical brown fat in humans: Development of a novel human fetal brown stem cell model. *Stem Cells.* 2016.

**55.** Fisher FM, Maratos-Flier E. Understanding the physiology of FGF21. *Annu Rev Physiol.* 2016;78:223-241.

**56.** Gunawardana SC, Piston DW. Insulin-independent reversal of type 1 diabetes in nonobese diabetic mice with brown adipose tissue transplant. *Am J Physiol Endocrinol Metab.* 2015;308:E1043-E1055.

**57.** Wang G-X, Zhao X-Y, Meng Z-X, et al. The brown fat–enriched secreted factor Nrg4 preserves metabolic homeostasis through attenuation of hepatic lipogenesis. *Nat Med.* 2014;20:1436-1443.

## FIGURES

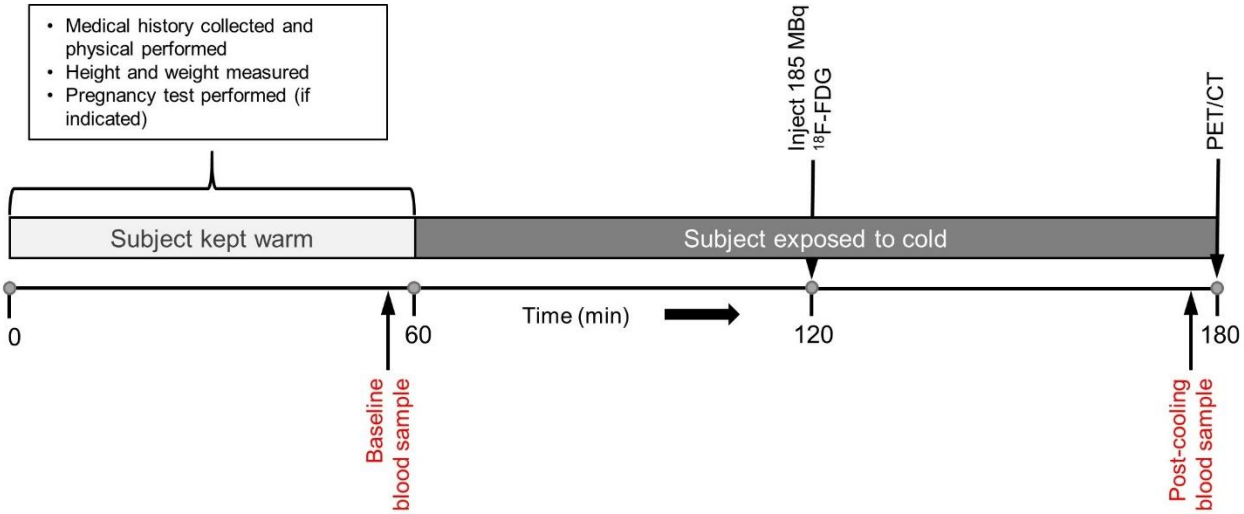


**Figure 1**. BAT activation and imaging process. Following a 1 h warming period, volunteers were cold-exposed for approximately 2 h to activate BAT. After 1 h of cooling, 185 MBq FDG was administered intravenously and PET/CT imaging was performed 60 min later, immediately following the cooling procedure.

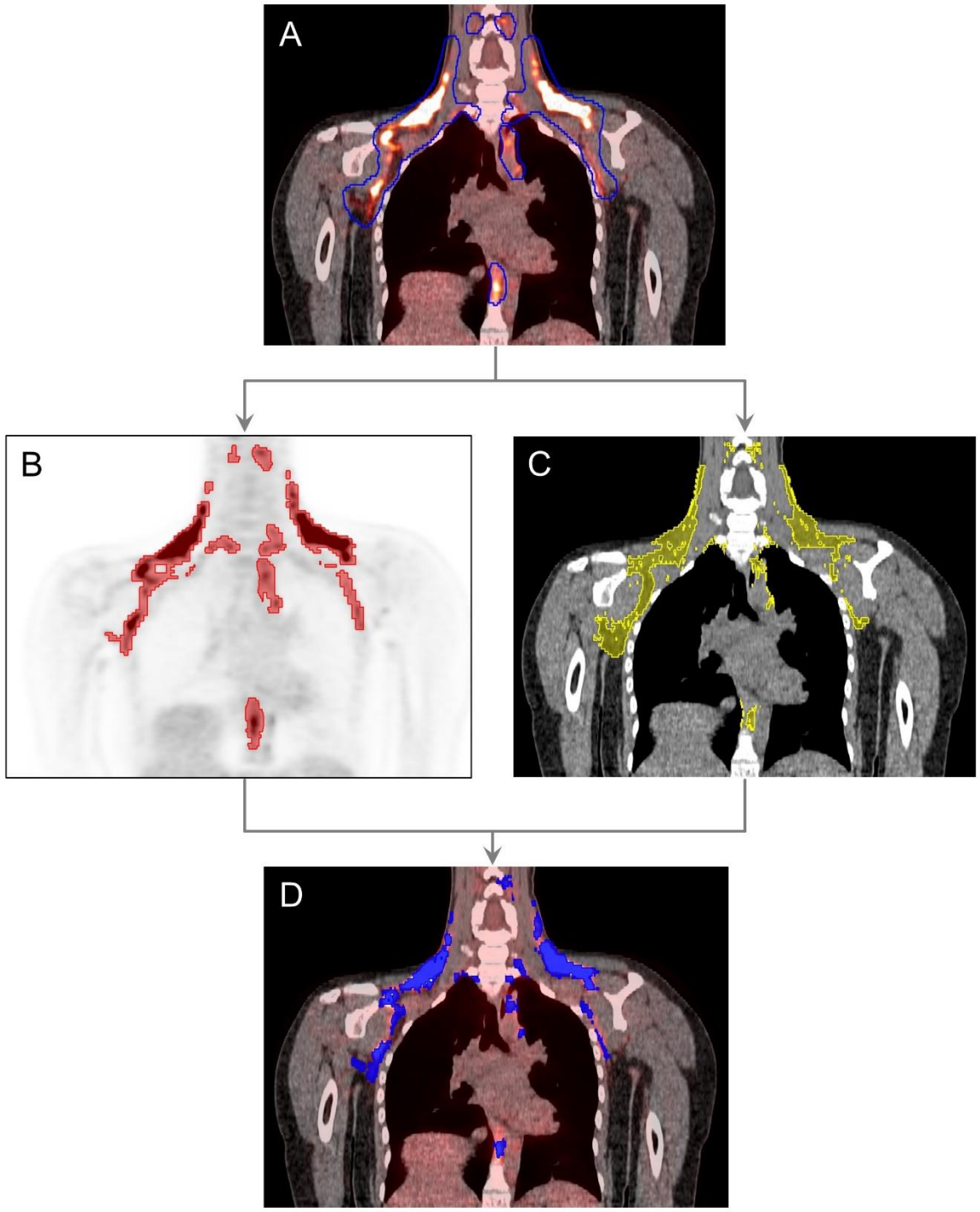


520

521 **Figure 2.** BAT segmentation was performed per the BARCIST 1.0 guidelines. Areas known to
522 contain BAT depots were manually delineated (A). On PET images, voxels with an SULMAX
523 less than 1.2 were removed (B) and On CT images, voxels with Hounsfield units outside a
524 range of -190 to -10 were removed (C). The Boolean intersection of the PET and CT images
525 was used to obtain final volumes of interest (D).
526

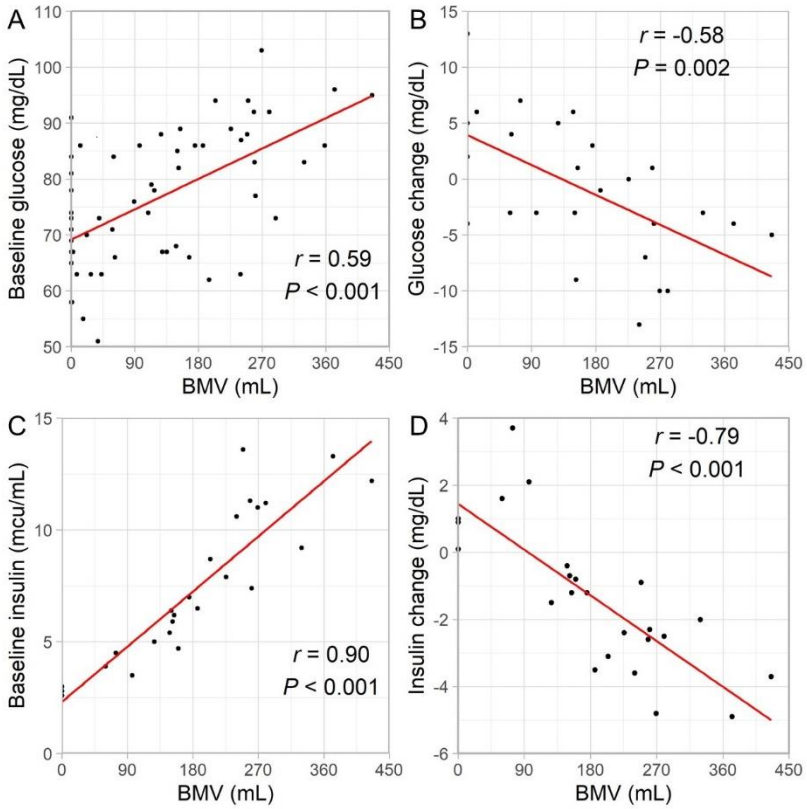


**Figure 3**. Regression analysis shows the correlation between BMV and baseline serum glucose (A), change in glucose from baseline to post-cooling (B), baseline serum insulin (C), and change in insulin (D). Baseline values were subtracted from post-cooling values.

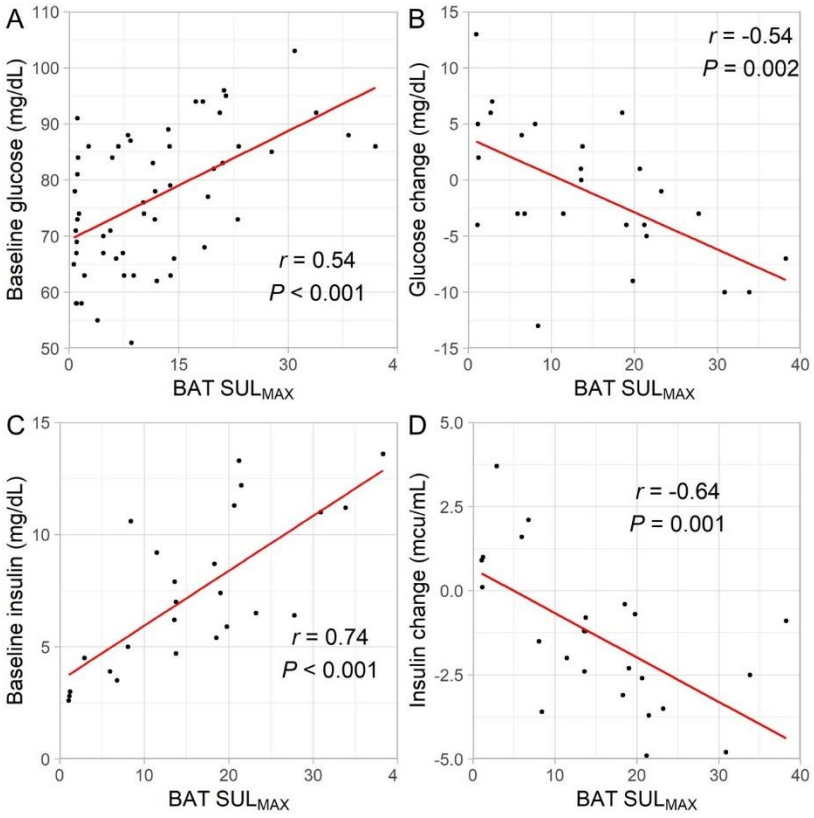


**Figure 4**. Regression analysis shows the correlation between BAT $SUL_{MAX}$ and baseline serum glucose (A), change in glucose from baseline to post-cooling (B), baseline serum insulin (C), and change in insulin (D). Baseline values were subtracted from post-cooling values.

## TABLES

**Table 1**. Subject characteristics. Values reported as frequency or mean ± SD. BAT volumes of 120 ml or more were defined as $BAT_{HIGH}$.

| | Total | $BAT_{HIGH}$ | $BAT_{LOW}$ |
|---|---|---|---|
| Gender (M/F) | 7/34 | 4/17 | 3/17 |
| Age (yr) | 23.8 ± 3.5 | 23.2 ± 2.7 | 24.7 ± 4.3 |
| Height (m) | 1.66 ± 0.09 | 1.67 ± 0.09 | 1.65 ± 0.09 |
| Weight (kg) | 62.3 ± 8.8 | 64.6 ± 9.1 | 59.6 ± 7.9 |
| BMI ($kg/m^2$) | 22.3 ± 1.8 | 23.0 ± 1.7 | 21.6 ± 1.5 |
| Race | | | |
| *White* | 20 | 12 | 8 |
| *Black* | 2 | 0 | 2 |
| *Asian* | 12 | 5 | 7 |
| Ethnicity | | | |
| *Hispanic* | 2 | 1 | 1 |
| *Non-Hispanic* | 32 | 16 | 16 |

**Table 2.** Glucose and insulin *t*-test and regression analysis results.

| Metabolite | Time-Point | μ ($BAT_{LOW}$) | σ | μ ($BAT_{HIGH}$) | σ | r (BMV) | r ($SUL_{MAX}$) | *P** |
|---|---|---|---|---|---|---|---|---|
| Insulin (mcu/ml) | Baseline | 3.3 | 0.8 | 8.7 | 3.0 | 0.90 | 0.74 | < 0.001 |
| | Post-Cooling | 4.9 | 1.9 | 6.1 | 2.6 | 0.71 | 0.43 | 0.327 |
| | Change | 1.6 | 1.2 | -2.7 | 1.4 | -0.79 | -0.64 | < 0.001 |
| Glucose (mg/dl) | Baseline | 70.8 | 10.2 | 88.3 | 11.4 | 0.59 | 0.54 | < 0.001 |
| | Post-Cooling | 84.3 | 12.3 | 85.2 | 7.3 | 0.12 | 0.06 | 0.815 |
| | Change | 3.0 | 5.6 | -3.1 | 5.5 | -0.58 | -0.54 | 0.013 |

**P*-values were generated using unpaired *t*-tests comparing $BAT_{HIGH}$ and $BAT_{LOW}$ groups. Using a Bonferroni correction, a P-value less than 0.025 was considered significant.

**Table 3.** Serum lipid *t*-test and regression analysis results.

| Lipid | Time-Point | μ ($BAT_{LOW}$) | σ | μ ($BAT_{HIGH}$) | σ | r (BMV) | r ($SUL_{MAX}$) | *P** |
|---|---|---|---|---|---|---|---|---|
| Cholesterol (mg/dl) | Baseline | 164.0 | 34.0 | 141.9 | 19.8 | -0.43 | -0.42 | 0.002 |
| | Post-Cooling | 174.0 | 32.4 | 156.0 | 21.2 | -0.34 | -0.34 | 0.010 |
| | Change | 9.0 | 11.0 | 14.9 | 7.9 | 0.33 | 0.26 | 0.023 |
| Triglycerides (mg/dl) | Baseline | 63.6 | 24.1 | 89.6 | 26.7 | 0.56 | 0.45 | < 0.001 |
| | Post-Cooling | 66.5 | 24.5 | 105.7 | 31.2 | 0.60 | 0.48 | < 0.001 |
| | Change | 4.5 | 12.2 | 15.7 | 13.2 | 0.45 | 0.34 | < 0.001 |
| HDL (mg/dl) | Baseline | 66.5 | 14.4 | 56.0 | 16.4 | -0.41 | -0.35 | 0.004 |
| | Post-Cooling | 70.6 | 13.6 | 62.4 | 20.9 | -0.28 | -0.22 | 0.181 |
| | Change | 3.4 | 4.9 | 6.4 | 12.0 | 0.21 | 0.23 | 0.231 |
| LDL (mg/dl) | Baseline | 83.7 | 28.9 | 73.8 | 21.3 | -0.16 | -0.23 | 0.058 |
| | Post-Cooling | 86.4 | 26.8 | 80.7 | 22.3 | -0.11 | -0.15 | 0.173 |
| | Change | -0.9 | 29.2 | 7.5 | 9.1 | 0.15 | 0.16 | 0.153 |
| NON-HDL (mg/dl) | Baseline | 97.2 | 29.5 | 89.2 | 19.5 | -0.14 | -0.19 | 0.093 |
| | Post-Cooling | 103.6 | 29.8 | 97.8 | 20.3 | -0.13 | -0.17 | 0.182 |
| | Change | 6.1 | 7.7 | 9.2 | 8.3 | 0.02 | 0.06 | 0.185 |

**P*-values were generated using unpaired *t*-tests comparing $BAT_{HIGH}$ and $BAT_{LOW}$ groups. Using a Bonferroni correction, a *P*-value less than 0.010 was considered significant.

**Table 4**. Additional baseline serum metabolite *t*-test and regression analysis results.

| Metabolite | Time-Point | μ ($BAT_{LOW}$) | σ | μ ($BAT_{HIGH}$) | σ | r (BMV) | r ($SUL_{MAX}$) | *P** |
|---|---|---|---|---|---|---|---|---|
| TSH (mcI/ml) | Baseline | 1.6 | 0.7 | 2.8 | 2.1 | 0.52 | 0.64 | 0.002 |
| Sodium (mmol/l) | Baseline | 141.0 | 1.8 | 139.0 | 1.3 | -0.40 | -0.39 | < 0.001 |
| Potassium (mmol/l) | Baseline | 3.8 | 0.3 | 4.0 | 0.3 | 0.31 | 0.26 | 0.002 |
| Chloride (mmol/l) | Baseline | 102.5 | 2.1 | 103.3 | 3.0 | 0.14 | 0.31 | 0.329 |
| CO2 (mmol/l) | Baseline | 26.0 | 1.7 | 25.9 | 2.1 | 0.07 | -0.14 | 0.964 |
| Anion Gap (mmol/l) | Baseline | 12.4 | 2.4 | 9.7 | 1.8 | -0.51 | -0.53 | < 0.001 |
| BUN (mg/dl) | Baseline | 13.2 | 2.8 | 10.7 | 2.2 | -0.43 | -0.50 | < 0.001 |
| Creatinine (mg/dl) | Baseline | 0.8 | 0.1 | 0.8 | 0.1 | 0.14 | -0.08 | 0.654 |
| Calcium (mg/dl) | Baseline | 9.4 | 0.5 | 9.3 | 1.0 | -0.05 | -0.13 | 0.454 |
| Bilirubin (mg/dl) | Baseline | 0.6 | 0.3 | 0.4 | 0.3 | -0.30 | -0.37 | 0.447 |
| Protein (g/dl) | Baseline | 7.5 | 0.5 | 7.1 | 0.4 | -0.41 | -0.46 | 0.002 |
| Albumin (g/dl) | Baseline | 4.6 | 0.3 | 4.3 | 0.3 | -0.49 | -0.54 | < 0.001 |
| Alk phos (units/l) | Baseline | 57.3 | 17.3 | 45.2 | 13.7 | -0.35 | -0.44 | < 0.001 |
| ALT (units/l) | Baseline | 18.3 | 4.4 | 34.0 | 26.4 | 0.53 | 0.24 | 0.006 |
| AST (units/l) | Baseline | 21.9 | 4.2 | 29.7 | 12.8 | 0.58 | 0.32 | 0.006 |

**P*-values were generated using unpaired *t*-tests comparing $BAT_{HIGH}$ and $BAT_{LOW}$ groups. Using a Bonferroni correction, a *P*-value less than 0.003 was considered significant (indicated in red).

554 **GRAPHICAL ABSTRACT**

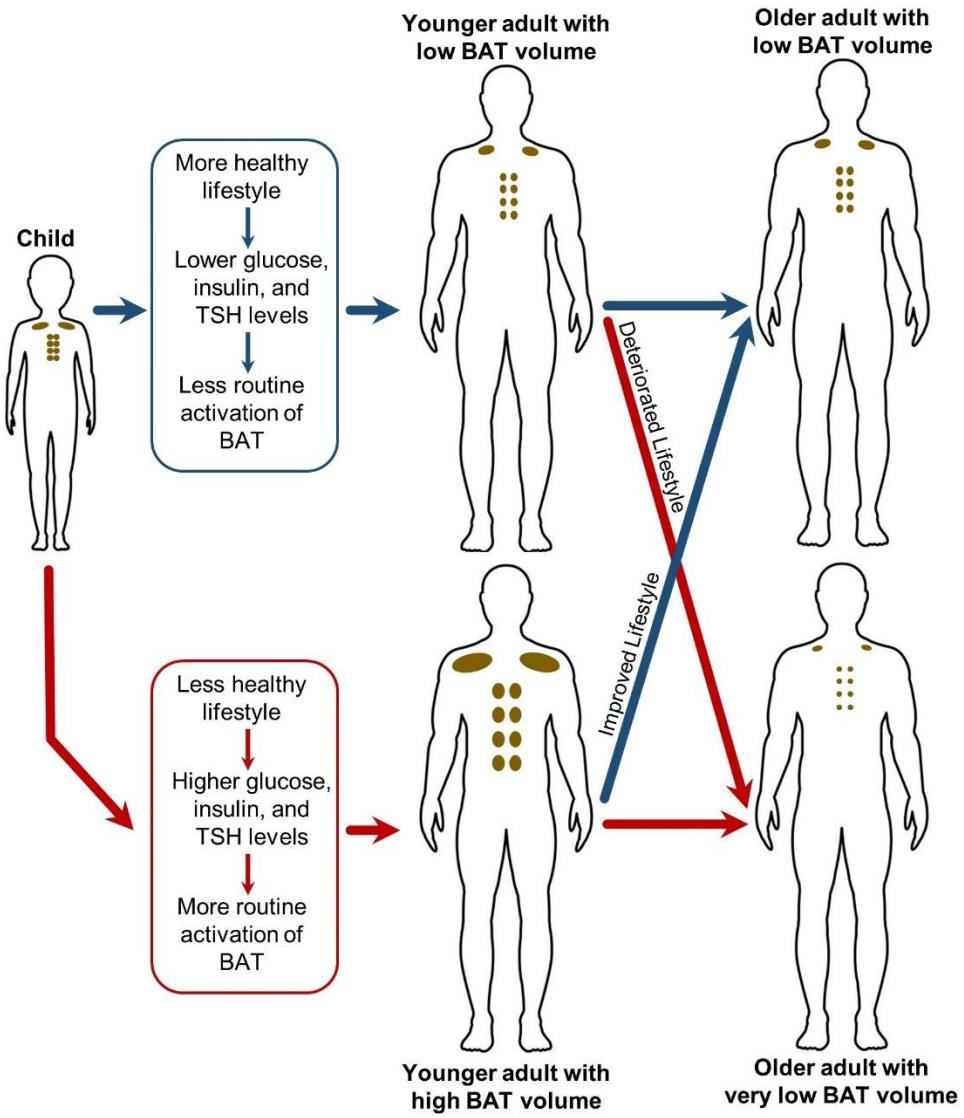


555

## Supplemental Figures

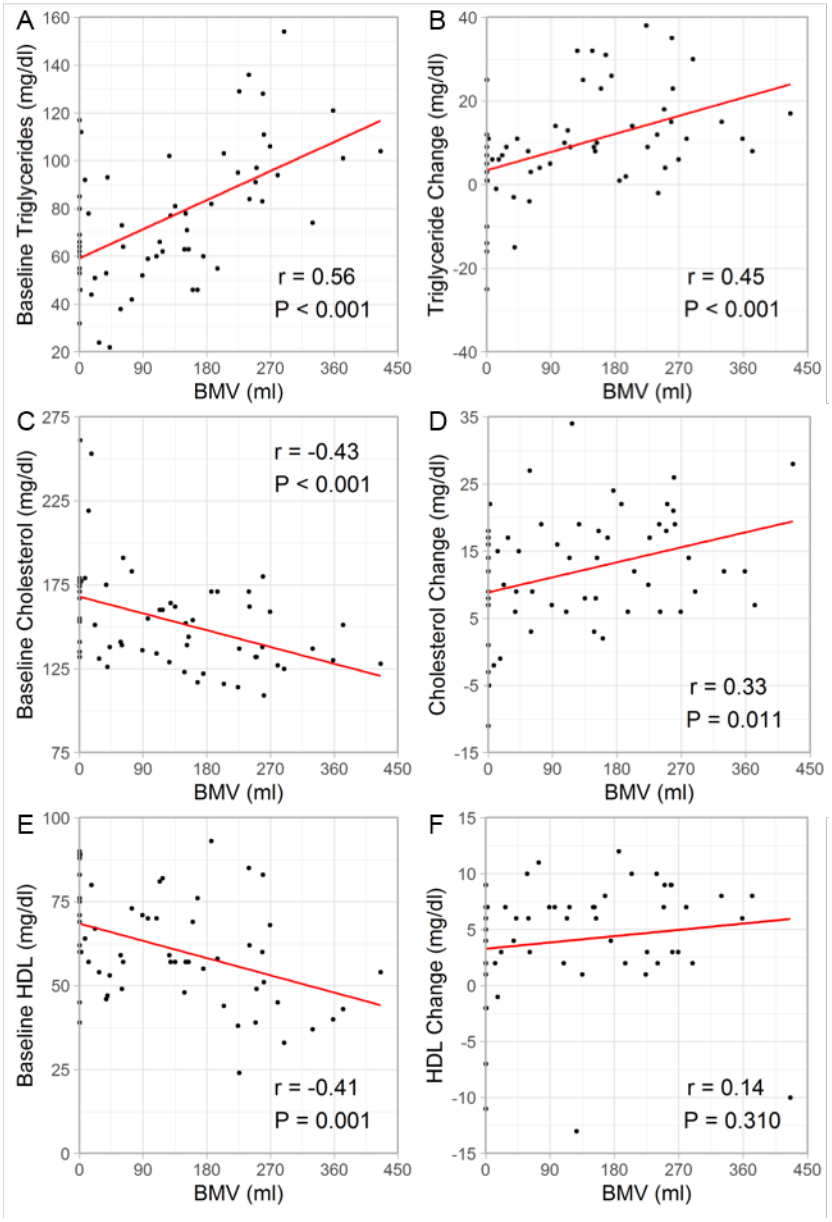


**Supplemental Figure 1**. Regression analysis shows the correlation between BMV and baseline serum triglycerides (A), change in triglycerides from baseline to post-cooling (B), baseline cholesterol (C), change in cholesterol (D), baseline HDL (E), and change in HDL (F). Baseline values were subtracted from post-cooling values.

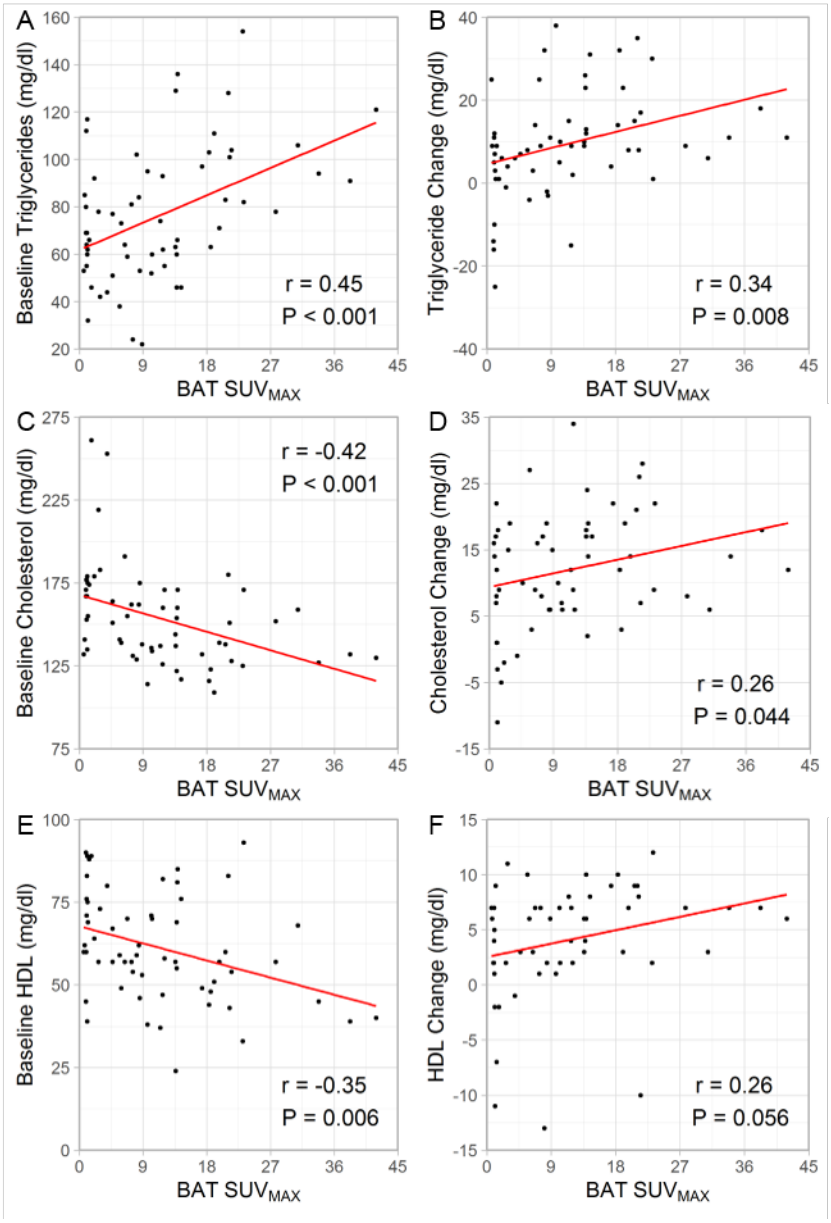


**Supplemental Figure 2**. Regression analysis shows the correlation between BAT $SUL_{max}$ and baseline serum triglycerides (A), change in triglycerides from baseline to post-cooling (B), baseline cholesterol (C), change in cholesterol (D), baseline HDL (E), and change in HDL (F). Baseline values were subtracted from post-cooling values.

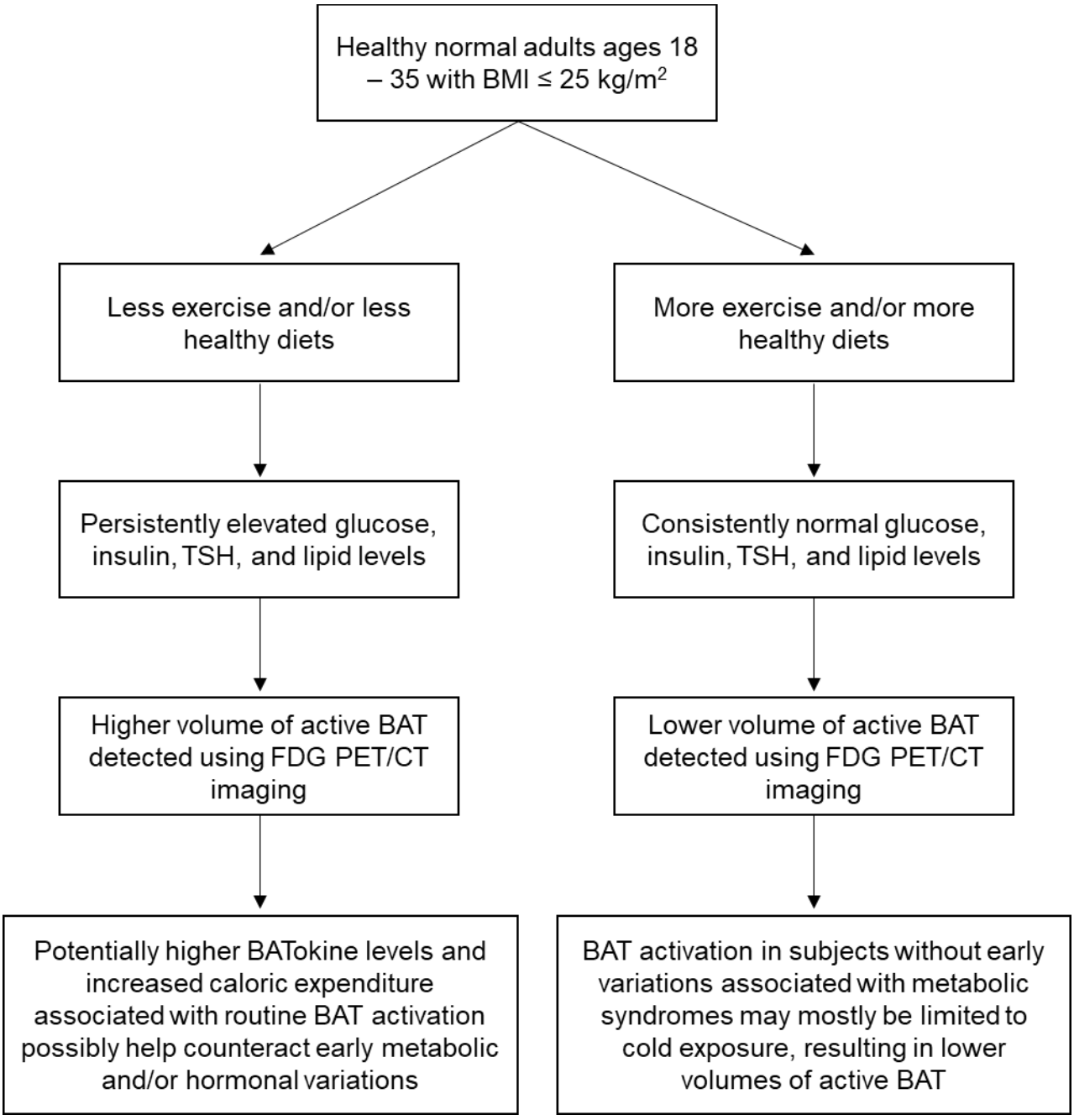


**Supplemental Figure 3.** This figure is intended to supplement the discussion and provide a potential explanation for the differences in metabolite levels in subjects with higher or lower volumes of active BAT.

**Supplemental Tables**

**Supplemental Table 1**. Eligibility Criteria.

| |
|---|
| Inclusion |
| • Age ≥ 18 and ≤ 35 years<br>• BMI ≤ 25 kg/$m^2$<br>• Ability to tolerate up to 80 min of imaging<br>• Ability and willingness to provide informed consent |
| Exclusion |
| • Uncontrolled intercurrent illness, including (but not limited to) active infections<br>• Current or prior habitual tobacco use d History of cold-related injury<br>• Insulin-dependent diabetes mellitus<br>• Use of medications that may interfere with brown fat activation (e.g., beta blockers)<br>• Metallic devices in the body, including (but not limited to) metallic joint prostheses, artificial heart valves, pacemakers, and cochlear implants<br>• Active pregnancy or nursing<br>• Inability to comply with study procedures |

**Supplemental Table 2**. FDG PET/CT Imaging and Reconstruction Parameters.

| Item | Description |
|---|---|
| Region of interest | Right Supraclavicular BAT Depot |
| Imaging modality | PET/CT |
| Scanner | Siemens Biograph 40 |
| Radiotracer | 18F-Fluorodeoxyglucose |
| Administered method | Intravenous injection |
| Scan type | Static imaging |
| Contrast agents | None |
| CT Parameters | |
| Tube current | 80 mAs max |
| Kilovoltage peak | 120 kVp |
| Pitch | 0.8 |
| Rotation time | 0.5 s |
| PET matrix size | 168 X 168 |
| PET slice thickness(mm) | 3mm |
| PET reconstruction method | OSEM with PSF |
| Iterations | 2 |
| Subsets | 21 |
| Smoothing Filter | 2 mm Gaussian |
| Attenuation correction | CT based |
| Randoms correction | Delayed event subtraction |
| Interpolation method | Trilinear |
| PET voxel size ($mm^3$) | 4.07 x 4.07 x 3.00 $mm^3$ |
| CT voxel size($mm^3$) | 0.98 x 0.98 x 3.00 $mm^3$ |

**Supplemental Table 3.** Serum Blood Sample Methods and Normal Ranges.

| Test | Methodology | Normal Low | Normal High | Units |
|---|---|---|---|---|
| Cholesterol | Enzymatic | 0 | 200 | mg/dL |
| Triglycerides | Enzymatic | 0 | 150 | mg/dL |
| HDL | Enzymatic | 60 | 180 | mg/dL |
| LDL | Calculated | 0 | 100 | mg/dL |
| Non-HDL | Calculated | 0 | 130 | mg/dL |
| Glucose | Enzymatic | 65 | 99 | mg/dL |
| Insulin | ECLIA | 2.6 | 25 | µIU/mL |
| TSH | ECLIA | 0.3 | 4.2 | µIU/mL |
| Sodium | ISE | 135 | 145 | mmol/L |
| Potassium | ISE | 3.3 | 4.9 | mmol/L |
| Chloride | ISE | 97 | 110 | mmol/L |
| $CO_2$ | Enzymatic | 22 | 32 | mmol/L |
| Anion Gap | Calculated | 2 | 15 | mmol/L |
| BUN | Colorimetric | 8 | 25 | mg/dL |
| Creatinine | Enzymatic | 0.6 | 1.3 | mg/dL |
| Calcium | Colorimetric | 8.5 | 10.3 | mg/dL |
| Bilirubin | Colorimetric | 0.1 | 1.2 | mg/dL |
| Protein | Colorimetric | 6.5 | 8.5 | g/dL |
| Albumin | Colorimetric | 3.5 | 5 | g/dL |
| Alkaline Phosphatase | Enzymatic | 40 | 130 | U/L |
| ALT | Enzymatic | 7 | 55 | U/L |
| AST | Enzymatic | 10 | 50 | U/L |

Abbreviations: HDL; high density lipoprotein, LDL; low density lipoprotein, ECLIA; electrochemiluminescence immunoassay, ISE; ion-selective electrode, TSH; thyroid stimulating hormone BUN; blood urea nitrogen, ALT; alanine aminotransferase, AST; aspartate aminotransferase.